

Article

Marine PET Hydrolase (PET2): Assessment of Terephthalate- and Indole-Based Polyester Depolymerization

Paula Wagner-Egea ^{1,†}, Lucía Aristizábal-Lanza ^{1,2}, Cecilia Tullberg ¹, Ping Wang ³, Katja Bernfur ⁴, Carl Grey ¹ , Baozhong Zhang ³  and Javier A. Linares-Pastén ^{1,*} 

¹ Division of Biotechnology, Department of Chemistry, Faculty of Engineering (LTH), Lund University, P.O. Box 124, SE-22100 Lund, Sweden

² Facultad de Ciencias, Universidad Nacional de Colombia, Sede Medellín, Medellín 050034, Colombia

³ Centre for Analysis and Synthesis, Department of Chemistry, Faculty of Engineering (LTH), Lund University, P.O. Box 124, SE-22100 Lund, Sweden

⁴ Division for Biochemistry and Structural Biology, Department of Chemistry, Lund University, P.O. Box 124, SE-22100 Lund, Sweden

* Correspondence: javier.linares_pasten@biotek.lu.se

† Current address: Center for Functional Protein Assemblies, Department of Chemistry, Technische Universität München, 85748 Garching, Germany.

Abstract: Enzymatic polyethylene terephthalate (PET) recycling processes are gaining interest for their low environmental impact, use of mild conditions, and specificity. Furthermore, PET hydrolase enzymes are continuously being discovered and engineered. In this work, we studied a PET hydrolase (PET2), initially characterized as an alkaline thermostable lipase. PET2 was produced in a fusion form with a 6-histidine tag in the N-terminal. The PET2 activity on aromatic terephthalate and new indole-based polyesters was evaluated using polymers in powder form. Compared with IsPETase, an enzyme derived from *Ideonella sakaiensis*, PET2 showed a lower PET depolymerization yield. However, interestingly, PET2 produced significantly higher polybutylene terephthalate (PBT) and polyhexylene terephthalate (PHT) depolymerization yields. A clear preference was found for aromatic indole-derived polyesters over non-aromatic ones. No activity was detected on Akestra™, an amorphous copolyester with spiroacetal structures. Docking studies suggest that a narrower and more hydrophobic active site reduces its activity on PET but favors its interaction with PBT and PHT. Understanding the enzyme preferences of polymers will contribute to their effective use to depolymerize different types of polyesters.

Keywords: plastic biodegradation; marine PET hydrolase; enzymatic degradation; indole-based polyesters; PETase; PET



Citation: Wagner-Egea, P.; Aristizábal-Lanza, L.; Tullberg, C.; Wang, P.; Bernfur, K.; Grey, C.; Zhang, B.; Linares-Pastén, J.A. Marine PET Hydrolase (PET2): Assessment of Terephthalate- and Indole-Based Polyester Depolymerization. *Catalysts* **2023**, *13*, 1234. <https://doi.org/10.3390/catal13091234>

Academic Editors: Maria Luisa Di Gioia, Luisa Margarida Martins and Isidro M. Pastor

Received: 27 June 2023

Revised: 10 August 2023

Accepted: 20 August 2023

Published: 24 August 2023



Copyright: © 2023 by the authors. Licensee MDPI, Basel, Switzerland. This article is an open access article distributed under the terms and conditions of the Creative Commons Attribution (CC BY) license (<https://creativecommons.org/licenses/by/4.0/>).

1. Introduction

Plastic materials are essential to society due to their wide range of applications. However, the vast production and use of fossil-based non-biodegradable plastics (≈99% of all plastics) has raised growing global concerns, including plastic littering and pollution, fossil dependence, and greenhouse gas emissions [1]. Recently, significant attention has been paid in academia and industry to developing effective plastics recycling technologies, including mechanical, chemical, and biological methods [2–4]. Notably, using microbes and enzymes for plastics recycling is attractive because of its milder and environmentally friendly conditions that can enhance sustainability [5].

Polyethylene terephthalate (PET) is a major plastic material widely used in packaging, beverage bottles, and textiles. The polymer structure consists of terephthalic acid and ethylene glycol units linked by ester bonds. Despite PET's resistance to biodegradation, several cutinase-like enzymes with PET-hydrolase activity have been discovered [3]. The enzymatic PET-hydrolysis was reported for the first time in 2005. A low crystallinity

(9%) PET was depolymerized up to 50% by using a thermostable hydrolase (TfH) from *Thermobifida fusca*, at 55 °C for three weeks [6]. Recently, other thermostable hydrolases have shown promising results. Without PET pre-treatment, a cutinase (HiC) from *Humicola insolens* has shown equal depolymerizing activity of amorphous and crystalline regions at 45 to 55 °C [7]. A modified form of compost metagenome-derived cutinase (LCC) depolymerized a pre-treated (amorphized and micronized) PET up to 90% in 10 h at 72 °C [8]. Recently, a PET-hydrolase (PET2) discovered in a marine metagenomic library that showed optimal activity between 55 and 70 °C and higher stability than the LCC at 90 °C [9] attracted our attention for assessing its activity in a series of different aromatic synthetic polymers (Figure 1).

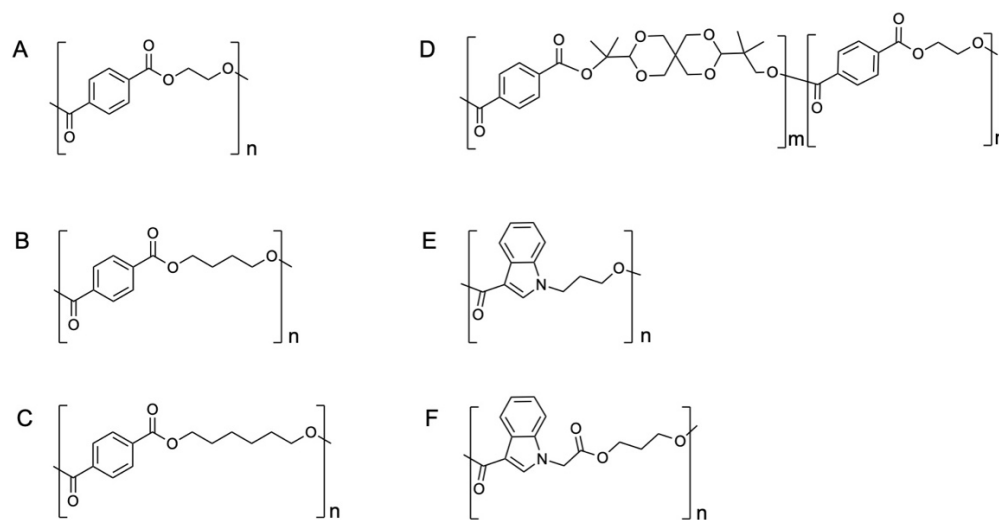


Figure 1. Assessed polyesters as potential substrates for the PET2 depolymerase. (A) PET, (B) PBT, (C) PHT, (D) Akestra™, (E) AB (aromatic), and (F) AABB (aliphatic aromatic).

Apart from PET, many another aromatic terephthalate homo- and co-polyesters are also widely used or gaining interest due to their physical and chemical properties. For instance, Akestra™ (Perstorp AB), a new terephthalate copolyester with spiroacetal structures, is an amorphous, durable polyester with potential use in hot-filling packaging [10,11]. Similar thermal and mechanical properties have also been achieved by using other rigid cyclic diols (e.g., 1,4-cyclohexanedimethanol, 2,2,4,4-tetramethyl-1,3-cyclobutanediol) in the production of terephthalate copolyesters (e.g., PETG, Tritan™ from Eastman). Furthermore, polybutylene terephthalate (PBT), synthesized from TPA (or DMT) and 1,4-butanediol, is used in electrical plug connectors, household devices such as irons, and sportswear [12,13]. Incorporating flexible adipic acid in the backbone of PBT resulted in a biodegradable polyester, PBAT, which has recently received considerable attention [14,15]. Polyhexamethylene terephthalate (PHT) has excellent potential in semiconductor materials and textiles [16–18].

Recently, the exploration of new aromatic polyesters with other potentially sustainable aromatic building blocks has been active, such as those with furan, indole, pyrazine, or various lignin-derived aromatics [19–25]. Particularly, sugar-based 2,5-furan-dicarboxylic acid (FDCA) has been intensively studied for the production of polyester, namely, poly(ethylene furanoate) (PEF), which shows similar thermal and mechanical properties, and even better barrier properties as PET and thus has potential to replace PET in the beverage bottles [26]. However, the relatively low thermal stability and discolouration during the polymerization of furan-based monomers have been a frequently countered challenge [27,28]. A lab-scale synthesis of bottle-grade PEF has been achieved using a complex three-step procedure [21]. Many other furan-based polyesters have also been reported on a lab scale [29]. In parallel to the rapid development of furan-based polyesters, some authors of this paper have been exploring the possibilities of developing polyesters based on indole, a larger aromatic unit.

Indole and many indole-derived aromatic molecules widely exist in nature and wastewater streams, which could also be produced by microorganisms [30]. It makes indole a potentially attractive aromatic building block for developing sustainable polymers. So far, several series of indole-based polyesters with different structures (e.g., flexibility, substitution patterns, type of ester bonds, and others) have been successfully synthesized, and their possibility to be degraded by enzymes has also been preliminarily demonstrated [31–34].

This article focuses on fundamental depolymerization studies and not directly on recycling. Therefore, the polymers used as enzyme substrates were prepared in powder form by dissolution-precipitation [35]. The PET2 activity on different aromatic terephthalate and indole-based polyesters was compared with the *Is*PETase activity on the same substrates. PET2, characterized initially as a lipase (lipIAF5-2) [36], has been recently suggested as another alternative for PET depolymerization, and thermostable mutants with improved activity have been developed [37]. However, to the best of our knowledge, the PET2 activity on polyesters other than PET is evaluated for the first time in this work.

2. Results and Discussion

2.1. Production of the Recombinant PET2

Recombinant PET2 was successfully produced in *E. coli* BL21(DE3). The yield was 0.3 g/L, and the estimated purity was more than 93%, according to the SDS-PAGE analysis (Figure 2A). However, the band observed in the gel, close to 25 kDa, did not match the molecular mass of the PET2. The average theoretical mass of the protein, including the tag in the N-terminal containing six histidines (MGSSHHHHHSSGLVPRGSH), is 30,258 Da. Therefore, the intact mass of the produced protein was analyzed by linear MALDI mass spectrometry, giving 30,419 Da (Figure 2B) using external calibration. This result indicates that PET2 was produced at its full length, and the band observed in the gel could be attributed to an anomalous migration.

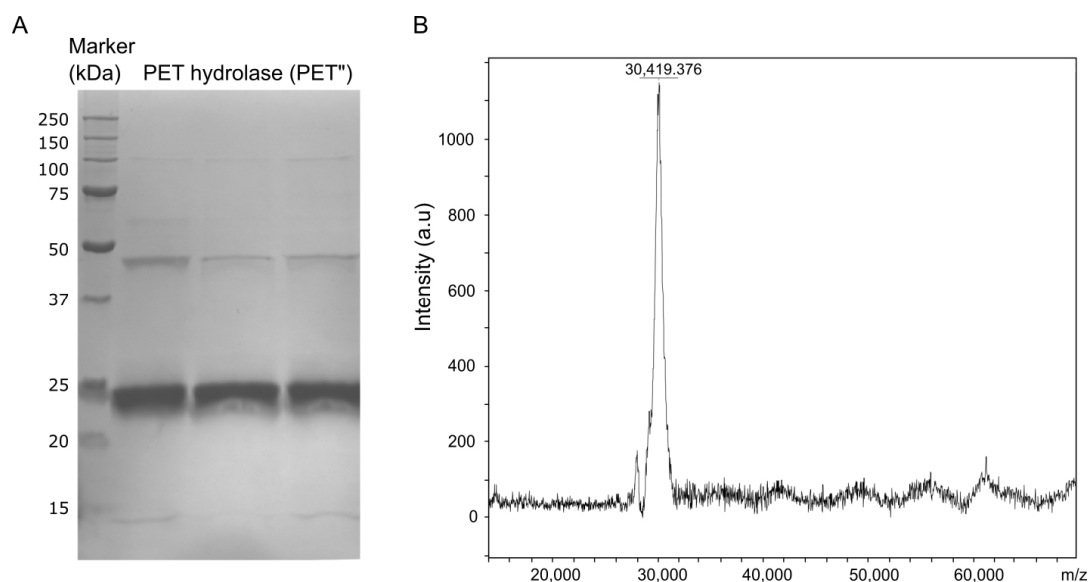


Figure 2. Purification and molecular weight analysis of PET2. (A) SDS-PAGE; notice that PET2 looks somewhat smaller than 25 kDa, which is attributed to an anomalous SDS-PAGE migration. (B) Linear MALDI mass spectrometry analysis of the same sample, intact PET2. Notice that the molecular weight was 30,419 Da, close to the theoretical determined mass of 30,258 Da.

2.2. PET2 Activity on Terephthalate Aromatic Polyesters

PET2 showed activity on PET, PBT, and PHT, while there was no activity on Akestra™. The highest activity was with PET, followed by PHT and PBT (Figure 3A). Compared to the *Is*PETase activity, both enzymes preferred PET with markedly higher *Is*PETase activity than PET2 under respective suitable pH and temperature conditions (Table 1). Both enzymes

showed similar product profiles, including TPA, mono-(2-hydroxyethyl) terephthalate (MHET), bis-(2-hydroxyethyl) terephthalate (BHET), and ethylene glycol (Figure 3B), which was also reported in other work [37]. However, PET2 showed greater activity than *IsPETase* on PBT and PHT. Regarding Akestra, *IsPETase* showed low activity, while no activity was detected for PET2 (Table 1), which significantly contrasts with the remarkable activity of HiC cutinase from *Humicola insolens* [38].

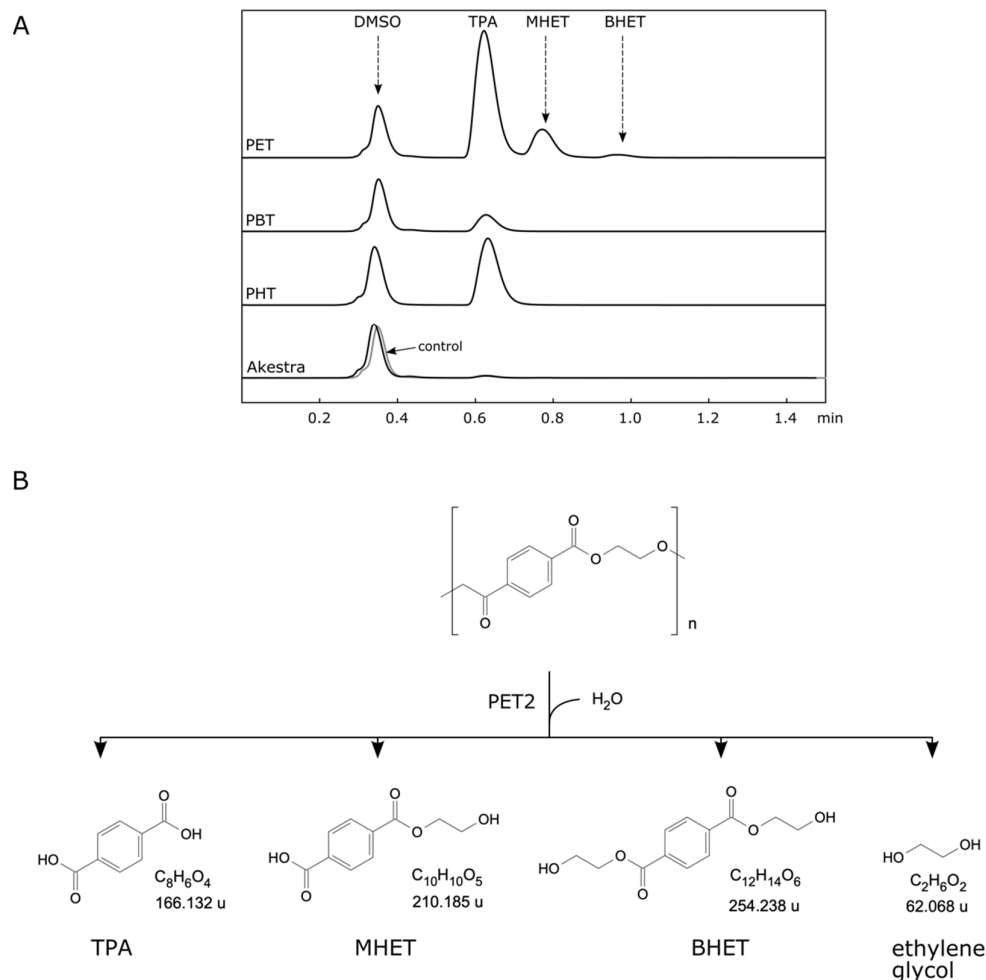


Figure 3. PET2 depolymerization activity on terephthalate polyesters. (A) HPLC analysis of PET2 depolymerization of terephthalate polyesters after 72 h: polyethylene terephthalate (PET), polybutylene terephthalate (PBT), polyhexamethylene terephthalate (PHT), and Akestra™. Notice that the tiny peak corresponding to TPA in the Akestra-depolymerization chromatogram was also present in the control. (B) PET depolymerization reaction. Notice that the ethylene glycol was not analysed, but it is a predicted product.

Table 1. Depolymerization of different terephthalate and indole-based polyesters after 72 h with PET2 at 55 °C, pH 9, and *IsPETase* at 37 °C, pH 7. The enzyme/substrate ratio was 0.07 mg/mg.

Polymer	PET2		<i>IsPETase</i> [35]	
	Degradation Products (mg/L)	Depolymerization (%)	Degradation Products (mg/L)	Depolymerization (%)
PET	1965	19.66	3934	39.34
PBT	138	1.38	25	0.25
PHT	974	9.74	12.5	0.13
Akestra™	N.D.	N.D.	13.3	0.13
AB	N.D.	N.D.		
AABB	925	7.01	N.Q.	N.Q.

N.D.—not detected; N.Q.—detected, but not quantified (below the quantification limit).

To further investigate the activity of PET2 and Trx-IsPETase against PET, initial reaction rates were obtained with incubation of a high enzyme/substrate ratio (1.12 mg/mg) for 4 h. The thioredoxin fusion domain (Trx) allowed a significant higher yield production of Trx-IsPETase than IsPETase and a positive effect on PET depolymerization [35]. Trx-IsPETase reached significantly higher activity than PET2, around five-fold (Figure 4A). Furthermore, the thermostability of both enzymes was also compared. The DSF analyses showed melting points (T_m) of 47.7 °C for Trx-IsPETase, and 56.7 °C for PET2 (Figure 4B). The T_m for PET2 determined here is significantly lower than the previously reported value in another work, 69 °C, by circular dichroism [37]. This difference can be attributed to several factors, mainly the use of different methods; additional amino acids from the histidine tag in the N-terminal of the construct (headline 2.1); and different buffer compositions, pH 9 here and pH 7 in the referenced work. The pH was chosen based on another work reporting PET2 preference in alkaline pH, from 8 to 9 [9]. No effect of calcium was detected by DSF analysis for either of the enzymes, which was consistent with the circular dichroism analysis reported previously [37]. The determined suitable temperature of 55 °C being so close to the T_m also indicates that the T_m determined by DSF might be underestimated, at least during operational conditions.

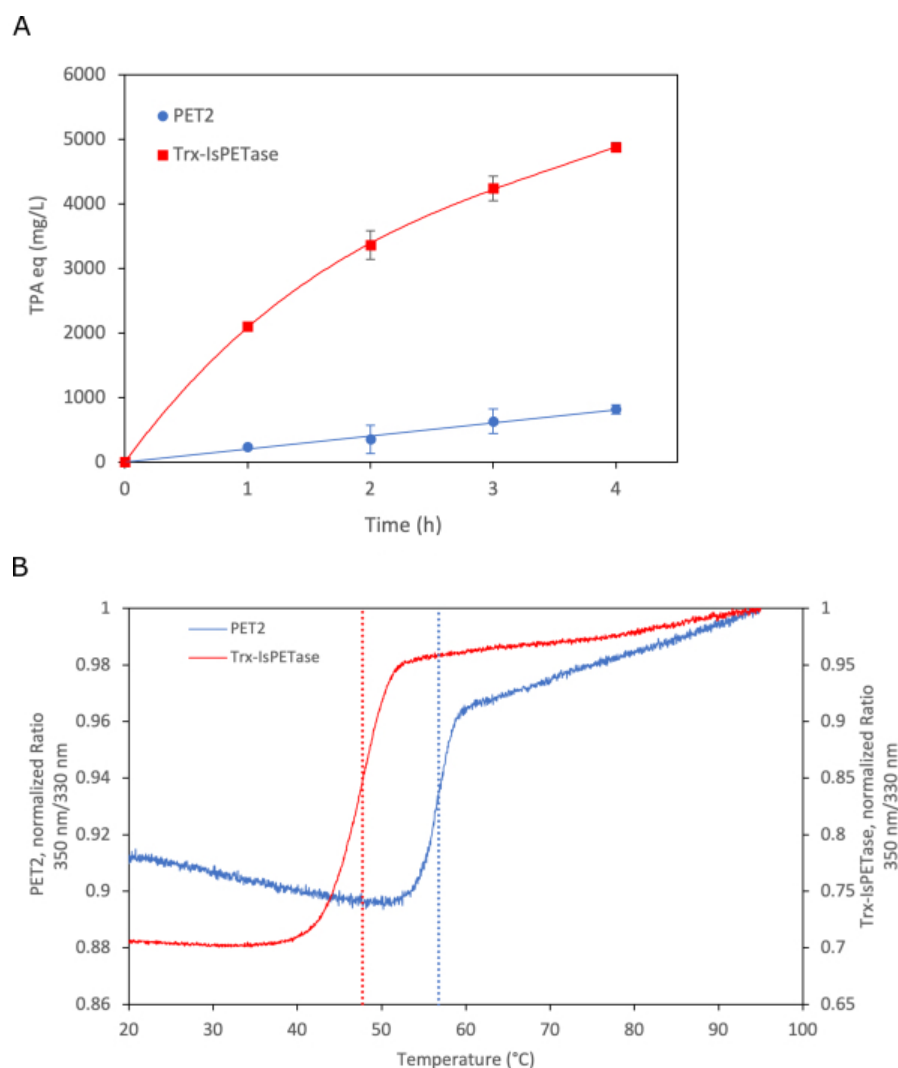


Figure 4. Compared reaction rates and melting points of PET2 and Trx-IsPETase. (A) Reaction rates of PET2 at 55 °C and Trx-IsPETase at 37 °C. The enzyme/substrate ratio was 0.12 mg/mg. (B) Melting points of PET2 and Trx-IsPETase; dotted lines represent melting points at 56.7 and 47.7 °C, respectively.

2.3. PET2 Activity on Indole-Based Polyesters

No PET2 activity was detected with polymer AB, while three depolymerization products were detected for AABB by LCMS (Figure 5). The main product was an indole monoester [2-(3-((3-hydroxypropoxy) carbonyl)-1H-indol-1-yl) acetic acid]; followed by an indole-diester [3-hydroxypropyl 1-(2-(3-hydroxypropoxy)-2-oxoethyl)-1H-indole-3-carboxylate]; and an indole-diacid [1-(carboxymethyl) indole-3-carboxylic acid], which was under the quantification limit of the HPLC analysis. The depolymerization products were quantified as equivalents in methyl 1-(2-methoxy-2-oxoethyl)-1H-indole-3-carboxylate, assuming that the extinction coefficient of the chromophore tryptophan group was the same as in the AABB depolymerization products. Thus, PET2 activity yielded ≈ 925 mg/L depolymerization products corresponding to $\approx 7\%$ of the polymer used as a substrate (Table 1).

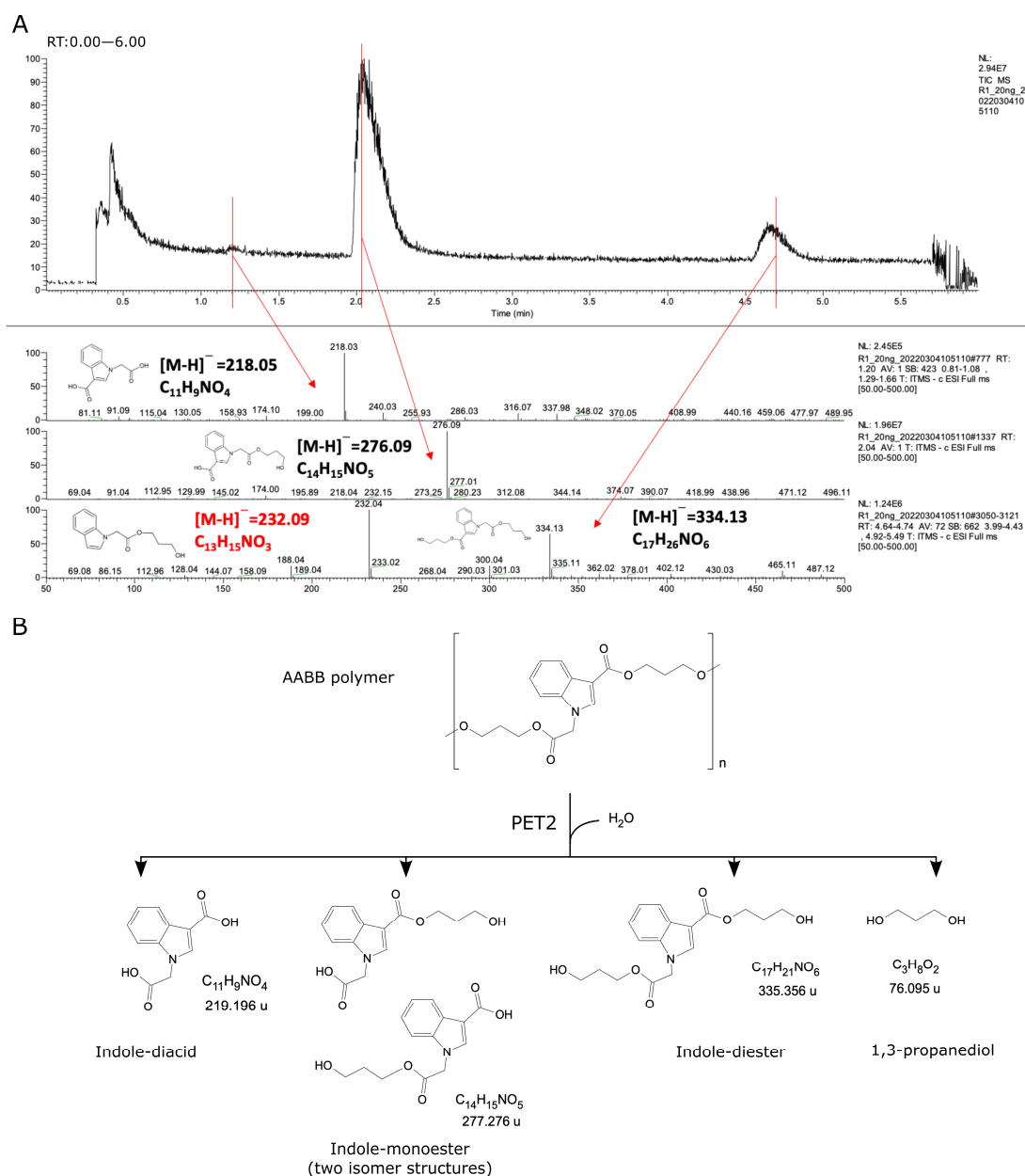


Figure 5. PET2 depolymerization activity on AABB polyester. (A) LCMS analysis of depolymerization products. (B) Proposed reaction based on the LCMS analysis. Notice that the 1,3-propanediol was not analyzed, but it is a predicted product from the AABB molecular structure. The molecule marked in red is not expected to be a main product based on the chemistry.

2.4. Structural Analysis

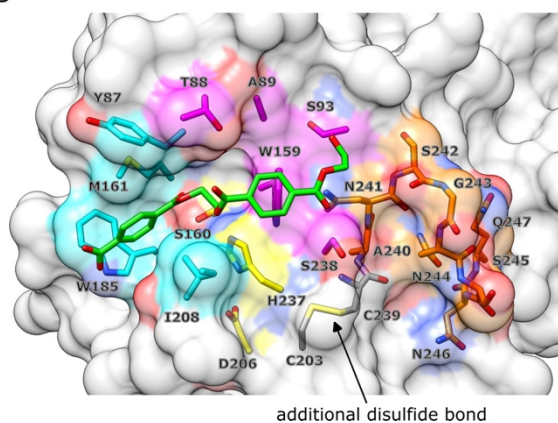
PET2 thermostability and its thermostabilized forms were recently reported by Nakamura et al. [37]. Therefore, the structural analysis performed in this work focused on comparing the active sites between *Is*PETase and PET2. PET-like enzymes were previously classified into two types, where type II enzymes were further subdivided into IIa and IIb [39]. This classification is based on a phylogenetic analysis of 69 putative PETases, as well as a comparative analysis of structures of *Is*PETase and cutinases active on PET. The catalytic amino acids Ser, His, and Asp are well conserved in all these enzymes, suggesting the same catalytic mechanism, independently of their thermal stability [40]. Ser is the nucleophile, His is the base, and Asp is the acid, as described for PET hydrolyzing enzymes [41]. The substrate cleavage point divides the binding cavity into subsites I and II. Type I and II PETases share the same key residues in subsite I but differ in subsite II. Furthermore, type II enzymes have an extended loop region connecting the β -strand 8 with the adjacent α -helix 5 and an additional disulfide bond linking this loop with the neighbouring β -strand 7 [40,42]. *Is*PETase is classified as type IIb due to the presence of a Ser132, while type IIa enzymes have Phe or Tyr instead [39]. Interestingly, PET2 does not fit very well within this classification system. PET2 has an extended loop but not an additional disulfide bond. In addition, PET2 has a Trp instead of Phe or Tyr in type IIa, or Ser in type IIb. It is also remarkable that the His229 of PET2 in the subsite I is also present in type I enzymes, such as PHL7, LCC, and TfCut2, while in *Is*PETase, it is Ser214 (Figure 6A). More structural and functional studies are needed to update the PETase classification system, but PET2 can be provisionally classified as a type II PETase.

A

Type	Enzyme	Catalytic triad			Subsite I								Subsite II				Extended loop region										
I	PHL7	S131	H209	D117	F63	M132	W156	I179	L93	Q95	H185	F189	T64	A65	S69	H130	L210	V211	S212	N213	T214	P215	D16	-	-	-	A174
II	PET2	S175	H253	D221	Y102	M176	W199	I223	Y132	Q134	H229	F233	L103	S104	S108	W174	W254	G255	A256	N257	G258	G259	N260	I261	Y262	S263	G219
IIb	<i>Is</i> PETase	S160	H237	D206	Y87	M161	W185	I208	L117	Q119	S214	I218	T88	A89	S93	W159	S238	C239	A240	N241	S242	G243	N244	S245	N246	Q247	C203

S
S
 additional disulfide bond

B



C

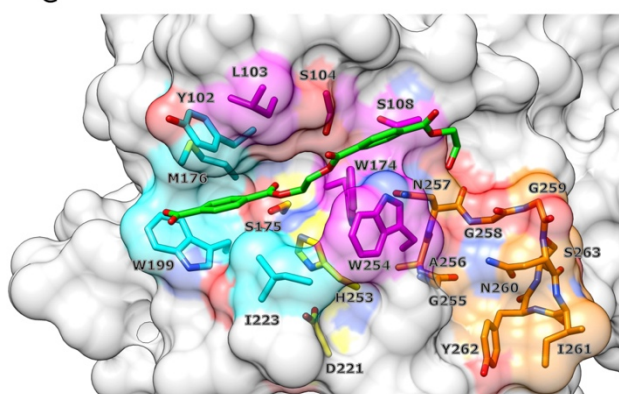


Figure 6. Subsites of *Is*PETase and PET2. (A) Alignments of structurally equivalent amino acids of *Is*PETase, PET2, and PHL7 (PDB ID: 8BRA). The catalytic triad is conserved in all enzyme types. The amino acids in subsite I that directly interact with the ligand are conserved (highlighted in cyan), while those in subsite II vary in several positions (in red). The extended loop is present in *Is*PETase and PET2 (type II enzymes), while not in PHL7 (type I). PET2 lacks an additional disulfide bond. (B) Surface representation of the *Is*PETase/(MHET)₂ complex and (C) PET2/(MHET)₂. The ligand is represented by sticks (carbons in green and oxygens in red). Note that (MHET)₂ is in a *gauche* conformation in *Is*PETase, whereas it is in *trans* in PET2. Catalytic amino acids are in yellow, subsite I amino acids are cyan, subsite II amino acids are magenta, and the extended loop is in orange.

Dockings of *Is*PETase and PET2 with a mono-(2-hydroxyethyl) terephthalate dimer (MHET)₂ have shown different ligand conformations—the carboxyl-free end MHET unit bound to subsite I, while the glycol-free end MHET unit bound to subsite II. In *Is*PETase, the OC-CO dihedral angle of the ethylene glycol (EG) moiety adopted a *gauche* conformation. However, interestingly, in PET2, the OC-CO dihedral angle of the EG moiety adopted a *trans* conformation (Figure 6B,C). NMR studies have shown that *gauche* EG moieties predominate in amorphous PET, while *trans* do so in crystalline PET [43]. These results, among others, could contribute to explaining the remarkably higher activity of the *Is*PETase than PET2 using as a substrate a highly amorphous PET (11.3% crystallinity).

*Is*PETase and PET2 share 53% of identity when comparing their amino acid sequences, excluding the signal peptides. However, despite these differences, the active sites have several conserved amino acids (Figure 7). Thus, the catalytic triad in PET2, Ser175, His237, and Asp212 corresponds well to the positions of Ser160, His237, and Asp206 in *Is*PETase. The amino acids of the proposed oxyanion hole [39] are also well conserved in both enzymes, Tyr102 and Met176 in PET2 and Tyr87 and Met161 in *Is*PETase. Other amino acids that stabilize PET are Trp199 and Ile223 in PET2, corresponding to Trp185 and Ile208 in *Is*PETase [32,44]. The Trp has been proposed to make π - π interactions between its indole ring and the PET aromatic ring. These amino acids have shown similar interactions with other aromatic terephthalates (Figure 7B–D) and indole (Figure 7E) dimeric esters used as ligands for docking. The presence of Trp254 and Leu103 in PET2 instead of Ser238 and Thr88 in *Is*PETase, respectively (Figures 7A and 7B), is the main difference between their active sites. The bulkier side group of Trp254 forms a narrower groove in the active site of PET2 than in *Is*PETase, which could affect the access of the polymeric substrate, giving a lower PET depolymerization yield, which was supported experimentally (Table 1). It is also consistent with the non-detectable activity on Akestra™ with PET2, which has a rigid spiroglycol terephthalate linker group (Table 1). On the other hand, Leu103 increases the hydrophobicity in PET2 remarkably (Figure 7B), which could favor the interactions with long flexible terephthalate linkers, such as the diol moieties of PBT, PHT, and AABB (Figure 7C–E). Indeed, PET2 gave a higher depolymerization yield than *Is*PETase for these substrates (Table 1). Phe105 in PET2 could also contribute to additional hydrophobic interactions with large linker substrates, such as PBT and PHT (Figure 7C,D), or bulkier aromatic groups, such as the indole group of AABB polymers (Figure 7E). The corresponding amino acid in *Is*PETase is Arg90. Although the docking studies can provide valuable information on PET hydrolases/ligands, more experimental support is still needed.

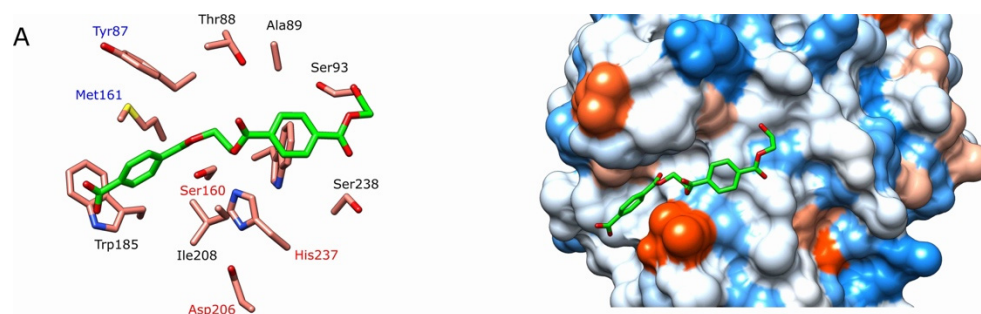


Figure 7. Cont.

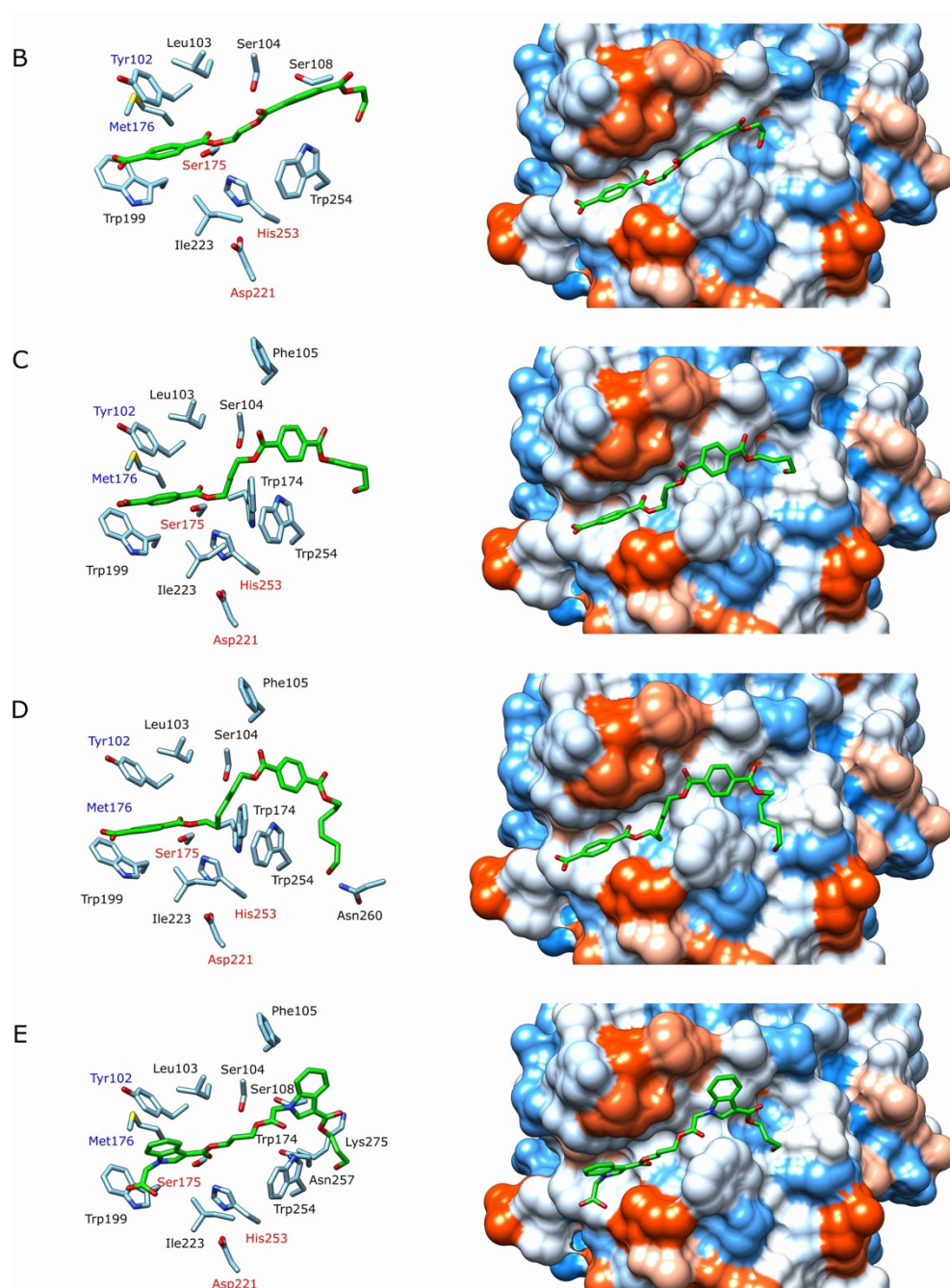


Figure 7. Docking of different ligands (represented in green) into PET2 and IsPETase. The hydrophobicity surfaces of the active sites are represented according to the Kyte–Doolittle scale, ranging from dodger blue for the most hydrophilic to white and to orange-red for the most hydrophobic [45]. Catalytic amino acids are labelled in red, while the suggested amino acids that stabilize the oxanion intermediate are in blue. (A) (MHET)₂/IsPETase (PDB ID:6EQE). (B) (MHET)₂/PET2. (C) (MHBT)₂/PET2. (D) (MHHT)₂/PET2. (E) (Indole-monoester)₂/PET2. Figure elaborated in UCSF Chimera v.1.15 [46].

3. Materials and Methods

3.1. Production and Purification of Recombinant PET2 and Trx-IsPETase

A recombinant intracellular PET2 enzyme was produced in the *Escherichia coli* BL21(DE3) strain. A synthetic gene encoding PET2 (GenBank accession number ON416993), with optimized codons, was inserted into the vector pET28b between the NdeI and XhoI restriction sites, giving the plasmid pET28b::PET2. The vector backbone provided a sequence

encoding a histidine tag at the N-terminus of PET2. *E. coli* BL21(DE3) harboring the plasmid was grown, at 37 °C, in 300 mL LB medium supplemented with kanamycin 35 mg/mL as a selection factor. The protein expression was induced with 1 mM IPTG and decreased to 20 °C when the optical density ($\lambda = 600$ nm) reached 0.6 for 20 h. Then, the cell pellets were separated by centrifugation at $5600 \times g$ for 10 min and washed with 30 mL of binding buffer (BB). PET2 was purified by immobilized metal affinity chromatography (IMAC), as described in our previous work [35], using a BB consisting of 100 mM Tris-HCl; 500 and mM NaCl adjusted to pH 7.4; and an elution buffer (EB) with the same composition as BB but with additional 500 mM imidazole, adjusted to pH 7.4. Recombinant Trx-IsPETase was also produced similarly and purified as described in our earlier work [35].

3.2. MALDI-TOF/TOF

MS spectrum of intact PET2 protein was acquired using an Autoflex Speed MALDI TOF/TOF mass spectrometer (Bruker Daltonics, Bremen, Germany) in positive linear mode. The protein sample was diluted 1:3 with 0.1% TFA (trifluoroacetic acid), and then 1 μ L of the sample was put on a MALDI target plate together with 0.5 μ L matrix solution consisting of 5 mg/mL α -cyano-4-hydroxy cinnamic acid, 80% acetonitrile, and 0.1% TFA. The spectrum was externally calibrated using intact BSA from Bruker Daltonics.

3.3. Polymer Preparation

Akestra™ was a courtesy from Perstorp AB; PET (Ramapet N180) was purchased from Indorama; PBT was purchased from Sigma-Aldrich, St. Louis, MO, USA; and PHT was synthesized according to a previously published protocol [47]. All the samples were prepared into powders by dissolution-precipitation as described previously [31,35]. Changes in crystallinity were assessed by differential scanning calorimetry [35,48]. Sample properties are summarized in Table 2.

Table 2. Properties of the polymers used before dissolution-precipitation, and crystallinity determined after dissolution-precipitation.

Polymer	IV * (dL/g)	T _g (°C)	T _m (°C)	M _n (g/mol)	M _w (g/mol)	Crystallinity (%)	Reference
PET	≈0.8	≈78	≈245			11.3	[35]
PBT			≈203	≈38,000		38.6	[35]
PHT	≈1.26	≈17	≈140	≈26,000	≈43,000	n.d.	[35]
Akestra™	≈0.64	≈95	-			Amorphous	[35]
AA		102	-	≈8100	≈14,500	Amorphous	[32]
AABB		93	-	≈35,800	≈71,700	Amorphous	[31]

* IV is intrinsic viscosity measured by GPC in chloroform; n.d. is not determined.

3.4. Enzymatic Reactions

The reaction mixtures were prepared in 2 mL vials. They consisted of 20 mg of prepared polymer, 50 mM buffer glycine/NaOH (pH 9), 2 mM CaCl₂, 10% DMSO, and 0.7 g/L of PET2. All reactions were performed in triplicates, for 72 h at 55 °C, and under shaking at 200 rpm. A negative control, including all components of the reaction except the enzyme, was incubated in the same conditions for each enzyme.

Reaction rates for PET2 and Trx-IsPETase were determined over a period of 4 h. The enzyme concentration was 0.12 g/L, and the substrate was 20 mg PET. The reaction conditions for PET2 were the same as described above, while for Trx-IsPETase were pH 7.4 and 37 °C, as described in our previous work [35]. The samples were taken every hour and analyzed by HPLC.

3.5. Reaction Products Analysis

The reaction products were analyzed by HPLC and LCMS following the methods previously developed [35]. Samples of 500 μ L were retrieved and diluted to 1:1 with DMSO. Afterwards, the dilutions were filtered and loaded in analytical vials. A hydrophobic

column C18 (Kinetex[®] 1.7 μm XB-C18 100 \AA , LC Column 50 \times 2.1 mm) was used with operational conditions described in a published paper [35]. The HPLC used was an Ultimate 3000 RS (Dionex, Sunnyvale, CA, USA), while the LCMS analysis was performed in an HPLC system (Thermo Fisher Scientific, Waltham, MA, USA) coupled to an LTQ Velos Pro Ion trap mass spectrum (Thermo Fisher Scientific) using a heated electrospray ionization source (HESI-II) operated in negative mode.

3.6. Differential Scanning Fluorometry

The thermal stability of both PET2 and Trx-*Is*PETase was evaluated by differential scanning fluorometry (DSF) using the Prometheus NT 48 nano DSF (NanoTemper Technologies GmbH, Munich, Germany). Samples, with or without 1 mM CaCl_2 , were prepared in 50 μL of a 50 mM buffer, Gly-NaOH for PET2 and phosphate buffer for Trx-*Is*PETase, and 1 mg/mL of the enzyme. Triplicates of 10 μL were loaded in the instrument capillaries and were heated from 20 to 90 $^\circ\text{C}$ at a rate of 1 $^\circ\text{C}$ per minute; then, to monitor protein unfolding, intrinsic fluorescence at emission wavelengths of 330 and 350 nm was analyzed.

3.7. Molecular Docking

PET2 was docked with ligands consisting of dimers of mono-(2-hydroxyethyl) terephthalate (MHET)₂, mono-(4-hydroxybutyl) terephthalate (MHBT)₂, mono-(6-hydroxyhexyl) terephthalate (MHHT)₂, (indole-monoester)₂, and *Is*PETase with (MHET)₂. The structure of the wild-type PET2 was obtained by reverse mutation of the crystal structure of the mutant 2M [37] (PDB ID: 7EC8), using YASARA v21.12.19 [49], while the crystal structure 6EQE (PDB ID) of *Is*PETase was used as the receptor. All ligands were prepared in the Avogadro program [50], as described previously [51]. The molecular geometries were optimized using the force field MMFF94, with the steepest descent algorithm, 5000 steps and convergence of 10^{-7} . Dockings were performed with AutoDock Vina [52], considering the total flexibility of the ligands. The docking boxes search varied according to the ligand size: for (MHET)₂ and (MHBT)₂ was $22.52 \times 10.49 \times 12.30 \text{ \AA}^3$, for (MHET)₂ was $29.49 \times 12.74 \times 16.12 \text{ \AA}^3$, and for the (indole-monoester)₂ was $27.20 \times 11.14 \times 14.89 \text{ \AA}^3$. The corresponding binding scores were -6.1 , -3.9 , -6.2 , and -6.5 , respectively. The interactions between enzymes and ligands were analyzed in UCSF Chimera v.1.15 [46].

4. Conclusions

Although PET2 is significantly more thermostable than *Is*PETase, the latter showed remarkably higher PET-depolymerizing activity. However, interestingly, PET2 has yielded higher depolymerization products from PBT and PHT than *Is*PETase. While *Is*PETase was able to depolymerize Akestra[™], PET2 did not produce any detectable degradation products. The highest activity of *Is*PETase and the different product profiles suggest that the differences between the active sites of PET2 and *Is*PETase are more determinant than the thermostability for the depolymerization processes. On the other hand, PET2 is more selective for indole-based polyesters, being able to attack the AABB-type indole-based polyester with a 1:1 ratio of aromatic and aliphatic ester groups, while being unable to attack the AB-type indole-based polyester with purely aromatic ester groups. Finally, understanding the enzymatic preferences of polymers will contribute to the effective use of enzymes to depolymerize different types of polyesters.

Author Contributions: Conceptualization, J.A.L.-P. and B.Z.; methodology, P.W.-E., L.A.-L., C.T., P.W., K.B. and C.G.; software, P.W.-E. and J.A.L.-P.; validation, P.W.-E., L.A.-L., C.T., P.W., K.B. and C.G.; formal analysis, J.A.L.-P., P.W.-E., L.A.-L., C.T., K.B., C.G. and B.Z.; investigation, J.A.L.-P., P.W.-E., L.A.-L., P.W., C.G. and B.Z.; resources, J.A.L.-P. and B.Z.; writing—original draft preparation, P.W.-E. and J.A.L.-P.; writing, review and editing, all authors; supervision, J.A.L.-P. and B.Z.; project administration, J.A.L.-P.; funding acquisition, J.A.L.-P. and B.Z. All authors have read and agreed to the published version of the manuscript.

Funding: This research was funded by The Crafoord Foundation, grant number 2020-0774; the Swedish Foundation for Strategic Environmental Research (Mistra) through the “STEPS” project (No. 2016/1489); the Swedish Research Council for Sustainable Development FORMAS (No. 2021-01107); and the Royal Physiographic Society in Lund.

Data Availability Statement: The files of the models presented in this study are available on request from the corresponding author. Other data are available in the article.

Acknowledgments: We thank Maria Gourdon from the Lund Protein Production Platform (LP3) for her assistance in using the DSF instrument. We thank Åsa Halldén Björklund and Linda Zellner from Perstorp AB for providing Akestra™ samples.

Conflicts of Interest: The authors declare no conflict of interest.

References

1. Wilcox, C.; Van Seville, E.; Hardesty, B.D. Threat of plastic pollution to seabirds is global, pervasive, and increasing. *Proc. Natl. Acad. Sci. USA* **2015**, *112*, 11899–11904. [[CrossRef](#)]
2. Kumar, R.; Sadeghi, K.; Jang, J.; Seo, J. Mechanical, chemical, and bio-recycling of biodegradable plastic: A review. *Sci. Total Environ.* **2023**, *882*, 163446. [[CrossRef](#)]
3. Mankar, S.V.; Wahlberg, J.; Warlin, N.; Valsange, N.G.; Rehnberg, N.; Lundmark, S.; Jannasch, P.; Zhang, B. Short-Loop Chemical Recycling via Telechelic Polymers for Biobased Polyesters with Spiroacetal Units. *ACS Sustain. Chem. Eng.* **2023**, *11*, 5135–5146. [[CrossRef](#)]
4. Arza, C.R.; Wang, P.; Linares-Pastén, J.; Zhang, B. Synthesis, thermal, rheological characteristics, and enzymatic degradation of aliphatic polyesters with lignin-based aromatic pendant groups. *J. Polym. Sci. Part A Polym. Chem.* **2019**, *57*, 2314–2323. [[CrossRef](#)]
5. Nikiema, J.; Asiedu, Z. A review of the cost and effectiveness of solutions to address plastic pollution. *Environ. Sci. Pollut. Res.* **2022**, *29*, 24547–24573. [[CrossRef](#)] [[PubMed](#)]
6. Müller, R.J.; Schrader, H.; Profe, J.; Dresler, K.; Deckwer, W.D. Enzymatic degradation of poly (ethylene terephthalate): Rapid hydrolyse using a hydrolase from *T. fusca*. *Macromol. Rapid Commun.* **2005**, *26*, 1400–1405. [[CrossRef](#)]
7. Kaabel, S.; Therien, J.D.; Deschênes, C.E.; Duncan, D.; Friščić, T.; Auclair, K. Enzymatic depolymerization of highly crystalline polyethylene terephthalate enabled in moist-solid reaction mixtures. *Proc. Natl. Acad. Sci. USA* **2021**, *118*, e2026452118. [[CrossRef](#)]
8. Tournier, V.; Topham, C.; Gilles, A.; David, B.; Folgoas, C.; Moya-Leclair, E.; Kamionka, E.; Desrousseaux, M.-L.; Texier, H.; Gavalda, S. An engineered PET depolymerase to break down and recycle plastic bottles. *Nature* **2020**, *580*, 216–219. [[CrossRef](#)]
9. Danso, D.; Schmeisser, C.; Chow, J.; Zimmermann, W.; Wei, R.; Leggewie, C.; Li, X.; Hazen, T.; Streit, W.R. New insights into the function and global distribution of polyethylene terephthalate (PET)-degrading bacteria and enzymes in marine and terrestrial metagenomes. *Appl. Environ. Microbiol.* **2018**, *84*, e02773-17. [[CrossRef](#)]
10. Hufendiek, A.; Lingier, S.; Du Prez, F.E. Thermoplastic polyacetals: Chemistry from the past for a sustainable future? *Polym. Chem.* **2019**, *10*, 9–33. [[CrossRef](#)]
11. Hatti-Kaul, R.; Nilsson, L.J.; Zhang, B.; Rehnberg, N.; Lundmark, S. Designing biobased recyclable polymers for plastics. *Trends Biotechnol.* **2020**, *38*, 50–67. [[CrossRef](#)] [[PubMed](#)]
12. Wang, W.; Wu, F.; Lu, H.; Li, X.; Yang, X.; Tu, Y. A Cascade Polymerization Method for the Property Modification of Poly (butylene terephthalate) by the Incorporation of Isosorbide. *ACS Appl. Polym. Mater.* **2019**, *1*, 2313–2321. [[CrossRef](#)]
13. De Vos, L.; Van de Voorde, B.; Van Daele, L.; Dubrue, P.; Van Vlierberghe, S. Poly (alkylene terephthalate) s: From current developments in synthetic strategies towards applications. *Eur. Polym. J.* **2021**, *161*, 110840. [[CrossRef](#)]
14. Peng, B.-Y.; Zhang, X.; Sun, Y.; Liu, Y.; Chen, J.; Shen, Z.; Zhou, X.; Zhang, Y. Biodegradation and Carbon Resource Recovery of Poly (butylene adipate-co-terephthalate)(PBAT) by Mealworms: Removal Efficiency, Depolymerization Pattern, and Microplastic Residue. *ACS Sustain. Chem. Eng.* **2023**, *11*, 1774–1784. [[CrossRef](#)]
15. Yang, Y.; Min, J.; Xue, T.; Jiang, P.; Liu, X.; Peng, R.; Huang, J.-W.; Qu, Y.; Li, X.; Ma, N. Complete bio-degradation of poly (butylene adipate-co-terephthalate) via engineered cutinases. *Nat. Commun.* **2023**, *14*, 1645. [[CrossRef](#)]
16. Guo, Z.; Warlin, N.; Mankar, S.V.; Sidqi, M.; Andersson, M.; Zhang, B.; Nilsson, E. Development of Circularly Recyclable Low Melting Temperature Bicomponent Fibers toward a Sustainable Nonwoven Application. *ACS Sustain. Chem. Eng.* **2021**, *9*, 16778–16785. [[CrossRef](#)]
17. Qian, K.; Qiao, R.; Chen, S.; Luo, H.; Zhang, D. Enhanced permittivity in polymer blends via tailoring the orderliness of semiconductive liquid crystalline polymers and intermolecular interactions. *J. Mater. Chem. C* **2020**, *8*, 8440–8450. [[CrossRef](#)]
18. Hall, I.; Ibrahim, B. The structure and properties of poly (hexamethylene terephthalate): 1. The preparation, morphology and unit cells of three allomorphs. *Polymer* **1982**, *23*, 805–816. [[CrossRef](#)]
19. Pan, T.; Deng, J.; Xu, Q.; Zuo, Y.; Guo, Q.X.; Fu, Y. Catalytic Conversion of Furfural into a 2, 5-Furandicarboxylic Acid-Based Polyester with Total Carbon Utilization. *ChemSusChem* **2013**, *6*, 47–50. [[CrossRef](#)]
20. Amarasekara, A.S.; Nguyen, L.H.; Okorie, N.C.; Jamal, S.M. A two-step efficient preparation of a renewable dicarboxylic acid monomer 5, 5'-[oxybis (methylene)] bis [2-furancarboxylic acid] from d-fructose and its application in polyester synthesis. *Green Chem.* **2017**, *19*, 1570–1575. [[CrossRef](#)]

21. Rosenboom, J.-G.; Hohl, D.K.; Fleckenstein, P.; Storti, G.; Morbidelli, M. Bottle-grade polyethylene furanoate from ring-opening polymerisation of cyclic oligomers. *Nat. Commun.* **2018**, *9*, 2701. [[CrossRef](#)] [[PubMed](#)]
22. Wang, G.; Xu, Y.; Jiang, M.; Wang, R.; Wang, H.; Liang, Y.; Zhou, G. Fully bio-based polyesters poly (ethylene-co-1, 5-pentylene 2, 5-thiophenedicarboxylate)s (PEPTs) with high toughness: Synthesis, characterization and thermo-mechanical properties. *Polymer* **2020**, *204*, 122800. [[CrossRef](#)]
23. Nguyen, H.T.H.; Reis, M.H.; Qi, P.; Miller, S.A. Polyethylene ferulate (PEF) and congeners: Polystyrene mimics derived from biorenewable aromatics. *Green Chem.* **2015**, *17*, 4512–4517. [[CrossRef](#)]
24. Gioia, C.; Banella, M.B.; Marchese, P.; Vannini, M.; Colonna, M.; Celli, A. Advances in the synthesis of bio-based aromatic polyesters: Novel copolymers derived from vanillic acid and ϵ -caprolactone. *Polym. Chem.* **2016**, *7*, 5396–5406. [[CrossRef](#)]
25. Wurdemann, M.A.; Bernaerts, K.V. Biobased Pyrazine-Containing Polyesters. *ACS Sustain. Chem. Eng.* **2020**, *8*, 12045–12052. [[CrossRef](#)]
26. Burgess, S.K.; Karvan, O.; Johnson, J.; Kriegel, R.M.; Koros, W.J. Oxygen sorption and transport in amorphous poly (ethylene furanoate). *Polymer* **2014**, *55*, 4748–4756. [[CrossRef](#)]
27. Terzopoulou, Z.; Karakatsianopoulou, E.; Kasmi, N.; Tsanaktsis, V.; Nikolaidis, N.; Kostoglou, M.; Papageorgiou, G.Z.; Lambropoulou, D.A.; Bikiaris, D.N. Effect of catalyst type on molecular weight increase and coloration of poly (ethylene furanoate) biobased polyester during melt polycondensation. *Polym. Chem.* **2017**, *8*, 6895–6908. [[CrossRef](#)]
28. Loos, K.; Zhang, R.; Pereira, I.; Agostinho, B.; Hu, H.; Maniar, D.; Sbirrazzuoli, N.; Silvestre, A.; Guigo, N.; Sousa, A. A Perspective on PEF Synthesis, Properties, and End-Life. *Front. Chem.* **2020**, *8*, 585. [[CrossRef](#)]
29. Tsanaktsis, V.; Terzopoulou, Z.; Exarhopoulos, S.; Bikiaris, D.N.; Achilias, D.S.; Papageorgiou, D.G.; Papageorgiou, G.Z. Sustainable, eco-friendly polyesters synthesized from renewable resources: Preparation and thermal characteristics of poly (dimethylpropylene furanoate). *Polym. Chem.* **2015**, *6*, 8284–8296. [[CrossRef](#)]
30. Ma, Q.; Zhang, X.; Qu, Y. Biodegradation and biotransformation of indole: Advances and perspectives. *Front. Microbiol.* **2018**, *9*, 2625. [[CrossRef](#)]
31. Wang, P.; Arza, C.R.; Zhang, B. Indole as a new sustainable aromatic unit for high quality biopolyesters. *Polym. Chem.* **2018**, *9*, 4706–4710. [[CrossRef](#)]
32. Wang, P.; Linares-Pastén, J.A.; Zhang, B. Synthesis, Molecular Docking Simulation, and Enzymatic Degradation of AB-Type Indole-Based Polyesters with Improved Thermal Properties. *Biomacromolecules* **2020**, *21*, 1078–1090. [[CrossRef](#)] [[PubMed](#)]
33. Arza, C.R.; Zhang, B. Synthesis, thermal properties, and rheological characteristics of indole-based aromatic polyesters. *ACS Omega* **2019**, *4*, 15012–15021. [[CrossRef](#)] [[PubMed](#)]
34. Wang, P.; Zhang, B. Sustainable aromatic polyesters with 1, 5-disubstituted indole units. *RSC Adv.* **2021**, *11*, 16480–16489. [[CrossRef](#)]
35. Wagner-Egea, P.; Tosi, V.; Wang, P.; Grey, C.; Zhang, B.; Linares-Pastén, J.A. Assessment of IsPETase-Assisted Depolymerization of Terephthalate Aromatic Polyesters and the Effect of the Thioredoxin Fusion Domain. *Appl. Sci.* **2021**, *11*, 8315. [[CrossRef](#)]
36. Meilleur, C.; Hupé, J.-F.; Juteau, P.; Shareck, F. Isolation and characterization of a new alkali-thermostable lipase cloned from a metagenomic library. *J. Ind. Microbiol. Biotechnol.* **2009**, *36*, 853–861. [[CrossRef](#)]
37. Nakamura, A.; Kobayashi, N.; Koga, N.; Iino, R. Positive charge introduction on the surface of thermostabilized PET hydrolase facilitates PET binding and degradation. *ACS Catal.* **2021**, *11*, 8550–8564. [[CrossRef](#)]
38. Aristizábal-Lanza, L.; Mankar, S.V.; Tullberg, C.; Zhang, B.; Linares-Pastén, J.A. Comparison of the enzymatic depolymerization of polyethylene terephthalate and AkestraTM using *Humicola insolens* cutinase. *Front. Chem. Eng.* **2022**, *4*, 1048744. [[CrossRef](#)]
39. Joo, S.; Cho, I.J.; Seo, H.; Son, H.F.; Sagong, H.-Y.; Shin, T.J.; Choi, S.Y.; Lee, S.Y.; Kim, K.-J. Structural insight into molecular mechanism of poly (ethylene terephthalate) degradation. *Nat. Commun.* **2018**, *9*, 382. [[CrossRef](#)]
40. Boneta, S.; Arafet, K.; Moliner, V. QM/MM Study of the Enzymatic Biodegradation Mechanism of Polyethylene Terephthalate. *J. Chem. Inf. Model.* **2021**, *61*, 3041–3051. [[CrossRef](#)]
41. Jerves, C.; Neves, R.P.; Ramos, M.J.; da Silva, S.; Fernandes, P.A. Reaction mechanism of the PET degrading enzyme PETase studied with DFT/MM molecular dynamics simulations. *ACS Catal.* **2021**, *11*, 11626–11638. [[CrossRef](#)]
42. Richter, P.K.; Blázquez-Sánchez, P.; Zhao, Z.; Engelberger, F.; Wiebeler, C.; Künze, G.; Frank, R.; Krinke, D.; Frezzotti, E.; Lihanova, Y. Structure and function of the metagenomic plastic-degrading polyester hydrolase PHL7 bound to its product. *Nat. Commun.* **2023**, *14*, 1905. [[CrossRef](#)] [[PubMed](#)]
43. Wei, R.; Song, C.; Gräsing, D.; Schneider, T.; Bielytskyi, P.; Böttcher, D.; Matysik, J.; Bornscheuer, U.T.; Zimmermann, W. Conformational fitting of a flexible oligomeric substrate does not explain the enzymatic PET degradation. *Nat. Commun.* **2019**, *10*, 5581. [[CrossRef](#)] [[PubMed](#)]
44. Sagong, H.-Y.; Seo, H.; Kim, T.; Son, H.F.; Joo, S.; Lee, S.H.; Kim, S.; Woo, J.-S.; Hwang, S.Y.; Kim, K.-J. Decomposition of the PET film by MHEase using Exo-PETase function. *ACS Catal.* **2020**, *10*, 4805–4812. [[CrossRef](#)]
45. Kyte, J.; Doolittle, R.F. A simple method for displaying the hydrophobic character of a protein. *J. Mol. Biol.* **1982**, *157*, 105–132. [[CrossRef](#)]
46. Pettersen, E.F.; Goddard, T.D.; Huang, C.C.; Couch, G.S.; Greenblatt, D.M.; Meng, E.C.; Ferrin, T.E. UCSF Chimera—A visualization system for exploratory research and analysis. *J. Comput. Chem.* **2004**, *25*, 1605–1612. [[CrossRef](#)]

47. Warlin, N.; Gonzalez, M.N.G.; Mankar, S.; Valsange, N.G.; Sayed, M.; Pyo, S.-H.; Rehnberg, N.; Lundmark, S.; Hatti-Kaul, R.; Jannasch, P. A rigid spirocyclic diol from fructose-based 5-hydroxymethylfurfural: Synthesis, life-cycle assessment, and polymerization for renewable polyesters and poly (urethane-urea) s. *Green Chem.* **2019**, *21*, 6667–6684. [[CrossRef](#)]
48. Din, S.U.; Satti, S.M.; Uddin, S.; Mankar, S.V.; Ceylan, E.; Hasan, F.; Khan, S.; Badshah, M.; Beldüz, A.O.; Çanakçı, S.; et al. The Purification and Characterization of a Cutinase-like Enzyme with Activity on Polyethylene Terephthalate (PET) from a Newly Isolated Bacterium *Stenotrophomonas maltophilia* PRS8 at a Mesophilic Temperature. *Appl. Sci.* **2023**, *13*, 3686. [[CrossRef](#)]
49. Krieger, E.; Koraimann, G.; Vriend, G. Increasing the precision of comparative models with YASARA NOVA—A self-parameterizing force field. *Proteins Struct. Funct. Bioinform.* **2002**, *47*, 393–402. [[CrossRef](#)]
50. Hanwell, M.D.; Curtis, D.E.; Lonie, D.C.; Vandermeersch, T.; Zurek, E.; Hutchison, G.R. Avogadro: An advanced semantic chemical editor, visualization, and analysis platform. *J. Cheminform.* **2012**, *4*, 17. [[CrossRef](#)]
51. Li, X.; Ilk, S.; Linares-Pastén, J.A.; Liu, Y.; Raina, D.B.; Demircan, D.; Zhang, B. Synthesis, Enzymatic Degradation, and Polymer-Miscibility Evaluation of Nonionic Antimicrobial Hyperbranched Polyesters with Indole or Isatin Functionalities. *Biomacromolecules* **2021**, *22*, 2256–2271. [[CrossRef](#)] [[PubMed](#)]
52. Trott, O.; Olson, A.J. AutoDock Vina: Improving the speed and accuracy of docking with a new scoring function, efficient optimization, and multithreading. *J. Comput. Chem.* **2010**, *31*, 455–461. [[CrossRef](#)] [[PubMed](#)]

Disclaimer/Publisher’s Note: The statements, opinions and data contained in all publications are solely those of the individual author(s) and contributor(s) and not of MDPI and/or the editor(s). MDPI and/or the editor(s) disclaim responsibility for any injury to people or property resulting from any ideas, methods, instructions or products referred to in the content.